REVIEWS

# 18 years of science with the Hubble Space Telescope

Julianne J. Dalcanton[1,2]

**After several decades of planning, the Hubble Space Telescope (HST) was launched in 1990 as the first of NASA's Great Observatories. After a rocky start arising from an error in the fabrication of its main mirror, it went on to change forever many fields of astronomy, and to capture the public's imagination with its images. An ongoing programme of servicing missions has kept the telescope on the cutting edge of astronomical research. Here I review the advances made possible by the HST over the past 18 years.**

The impact of the HST on the public imagination is large, yet many are surprised to learn that the HST is rather modestly sized in comparison with modern telescopes (Fig. 1). Its mirror is only a generous arm span across, with less than ~1/15th the light-gathering area of the largest telescopes available on the ground. Its instruments are likewise far from state of the art, containing detectors whose technologies are sometimes more than a decade old. What then accounts for the HST's tremendous scientific and public impact?

The HST's successes can be attributed to the same three key factors influencing real estate: location, location, location. Raising the HST above most of the Earth's atmosphere has allowed it to escape a host of problems that limit telescopes on the ground. The first of the resulting improvements is the dramatic increase in a telescope's resolution—the smallest angular separation that can be reliably detected (Fig. 2). Images taken with the HST can distinguish features that are separated by less than a tenth of an arc second (comparable to the angle spanned by half a millimetre when seen from a kilometre away). Comparable images made from the ground are typically blurred by a factor of ten relative to those made with the HST. Moreover, because the HST's view of the Universe is unperturbed by the turbulent, chaotic atmosphere, the images and spectra taken by the telescope are stable and reproducible. This stability allows for an unprecedented level of precision when measuring the brightness and structure of astrophysical objects.

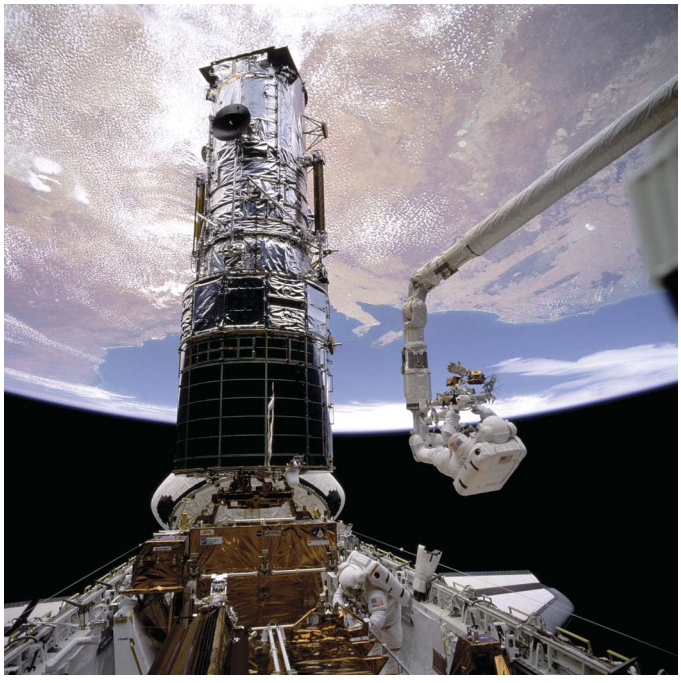

**Figure 1 | The Hubble Space Telescope, while docked with the Space Shuttle Endeavour during servicing.** The new instruments installed during such missions have kept HST at the cutting edge of astronomy. Image courtesy of NASA.

The second, less publicized benefit of the HST's location is the darkness of space-based imaging. From the ground, the night sky is not actually all that dark. Atoms in the upper atmosphere absorb energy from sunlight during the day, and then re-radiate that energy as light during the night. In much the same way that you can see more stars from a dark campground than from a bright city street, from space the HST can measure astronomical features fainter than those ground-based telescopes can detect against the glowing background of the night sky. This increase in contrast is especially pronounced at ultraviolet wavelengths, where photons are otherwise absorbed by the Earth's atmosphere and are thus inaccessible from the ground. Access to this portion of the electromagnetic spectrum is critical for tracing the abundance of individual elements in astrophysical gases, and for interpreting observations of galaxies at large distances.

In this article I summarize some of the many areas where the HST has dramatically changed our understanding of the Universe. These include tracing the structure and evolution of stars from their births through to their deaths, demonstrating the pervasiveness of black holes and their links to galaxy formation, tracking the evolution of galaxies over billions of years, and testing fundamental models of the expansion of the Universe.

## Distance scale

One of the most consistently vexing issues facing astronomers is measurement of the distances to astronomical objects. It perhaps seems odd that something so basic, and so easily judged on Earth, can be so difficult in an astronomical context. However, in astronomy we observe systems whose energy outputs and distances can differ by a dozen orders of magnitude. We therefore often have little a priori knowledge with which to estimate the basic size and energy

[1]University of Washington, Seattle, Washington 98195, USA. [2]Max-Planck-Institut für Astronomie, D-69117 Heidelberg, Germany.

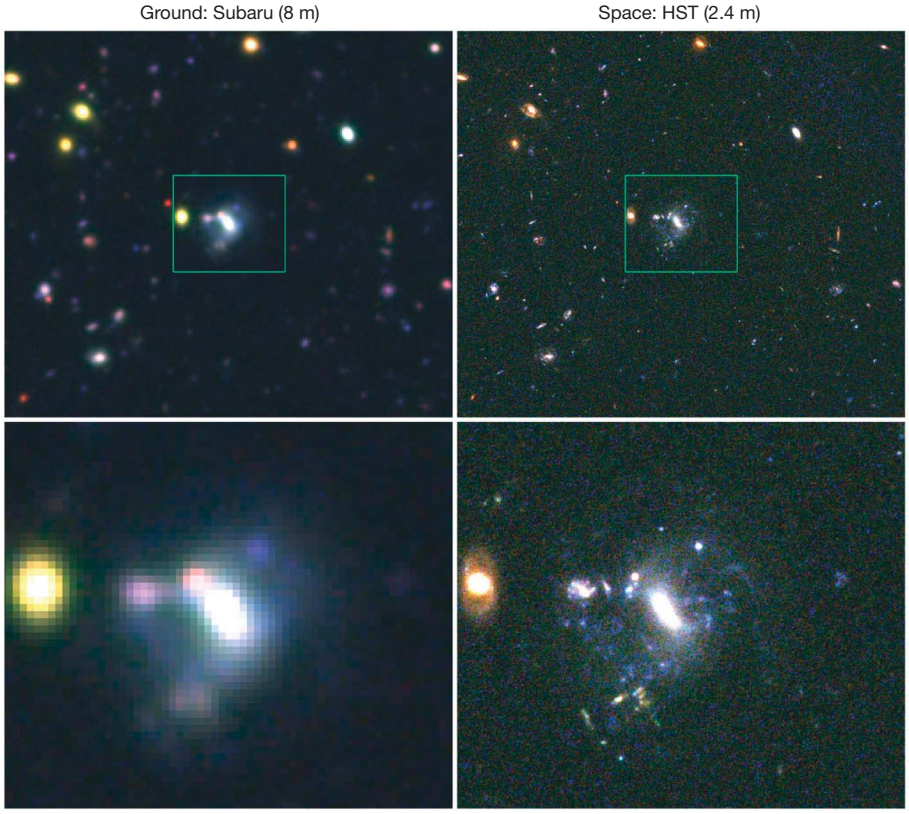


**Figure 2 | Images taken from space have superb spatial resolution.** Images of a distant galaxy taken from the ground (with the Subaru 8-m telescope (National Astronomical Observatory of Japan) on Mauna Kea) are blurred in comparison with images of the same galaxy made with the HST. Images courtesy of NASA.

scales of a given system. Are we observing a faint object that happens to be close, or a bright object that is much farther away? Moreover, even when we can make reasonable assumptions about an object's distance, we frequently lack the precision needed for critical cosmological tests.

Over the past century, astronomers have built up an elaborate distance 'ladder', which uses the distances to the nearest stars to infer the distances to more distant objects. We start the ladder with stars that are sufficiently close that their position on the sky shifts during the Earth's orbit around the Sun. This parallax effect (which you can see by alternately shutting your left and right eyes) can be used to calculate a distance on the basis of the principles of geometry only, making it robust against systematic errors. The only limit to the method is the precision with which we can measure slight angular shifts. With higher resolution, parallax measurements can be pushed to much larger distances.

The HST excels at parallax measurements owing to both its superb resolution and its Fine Guidance Sensor (FGS). Although the FGS is primarily responsible for keeping the telescope oriented precisely during scientific observations, it can also be used to make milli-arc-second measurements of the angular positions of individual stars. Moreover, the FGS is quite sensitive and can measure accurate parallaxes for stars that are much fainter than those that could be studied with the earlier parallax mission satellite HIPPARCOS (the High Precision Parallax Collecting Satellite). By measuring parallaxes of fainter stars, the HST can probe to larger distances, and sample a larger volume of the Galaxy. This allows the HST to calibrate the luminosities of truly rare stars which are difficult to find nearby, but that are crucial for establishing more distant rungs on the distance ladder.

One of the most important types of such stars are Cepheids, a class of pulsating stars that are up to thousands of times more luminous than the Sun, and can thus be identified in galaxies far outside the Milky Way owing to their brightnesses and characteristic periodic variations in luminosity. A Cepheid's luminosity is tightly correlated with the duration of its pulsation cycle. Once this correlation is calibrated, one can then deduce the distance to a Cepheid by measuring the duration of its pulsation, inferring its luminosity and then comparing the luminosity with the apparent brightness. The accuracy of the derived distance is typically limited by the accuracy of the initial period–luminosity relationship. The FGS on the HST has made direct parallax measurements of this relationship[1], greatly reducing the uncertainties in Cepheid-based distances. Although this period–luminosity relationship may potentially vary with the metallicity of the galaxy[2], with appropriate corrections it can reliably be used for many massive spiral galaxies. Previously, climbing from reliable parallax measurements of nearby stars to Cepheid-based distances to spiral galaxies required many complicated steps up the distance ladder. With the new HST results, astronomers can make this step in a single jump.

Identifying Cepheids in nearby galaxies requires the HST's resolution. Although Cepheids are luminous, they can appear to be blended together with the light from many other stars in images from ground-based telescopes, making it impossible to identify the luminosity fluctuations or the brightness of the one star in the cluster that happens to be a Cepheid. In contrast, the high angular resolution of

**Figure 3 | A montage showing the life cycle of stars. a**, The Orion nebula is a dense cloud of gas within which new stars are forming. The inset shows a close-up of a young star surrounded by a dusty disk that may eventually form planets. **b**, Young blue stars surrounded by leftover natal gas in the Large Magellanic Cloud, a nearby dwarf galaxy. **c**, The evolving star V838 Monocerotis, whose past flashes have illuminated material that was ejected in an early stellar wind. **d**, A planetary nebula forms as a dying star sheds its outer layers, leaving behind a fading white dwarf at its centre. **e**, A globular cluster containing many old stars. The faintest stars in the cluster are white dwarfs. Images courtesy of NASA.

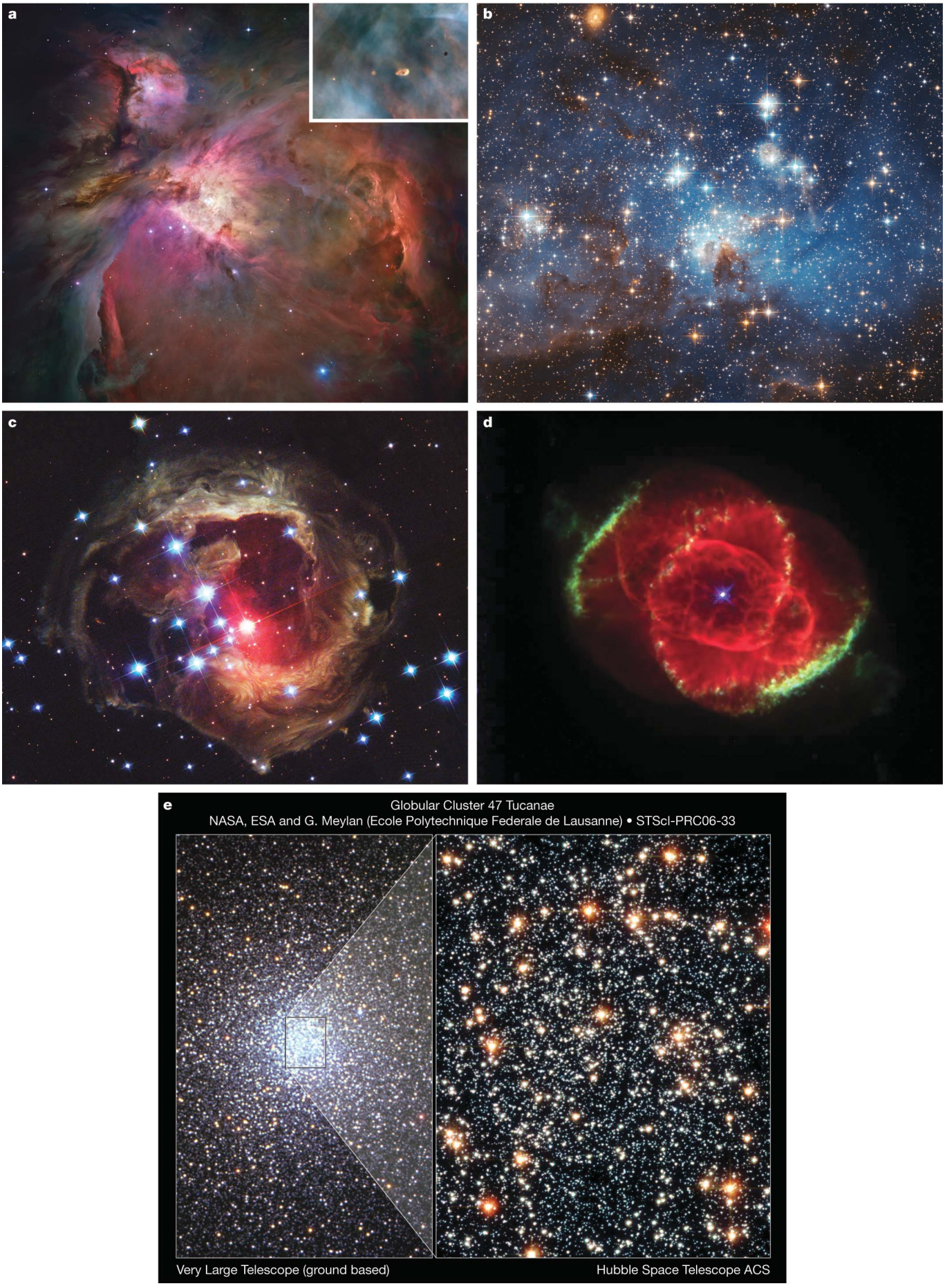

the HST allows Cepheids to be separated from their neighbouring stars out to vastly larger distances, increasing the number of galaxies with potentially reliable distances by a factor of close to 1,000. Establishing Cepheid-based distances to nearby galaxies was one of the Key Projects identified before the HST's launch. The Cepheid Key Project has since used hundreds of orbits to analyse Cepheids in 36 galaxies, all of which were used to calibrate even more distant rungs of the ladder (such as supernovae and the Tully–Fisher relationship).

These Cepheid distances have become the bedrock foundation of our understanding of the size scale of the distant Universe. Distances to galaxies can be inferred from the 'Hubble diagram'— a linear relationship between the distance to a galaxy and the speed at which it appears to be receding from us. The slope of this relationship is known as the Hubble constant, and once its value is known it is possible to measure recessional velocities to galaxies (which is straightforward) and use them to infer distances (which is difficult). The HST's observations of Cepheids have been essential in establishing the distance portion of the Hubble diagram, and thus have laid the foundations for modern measurements of the Hubble constant. Before the HST, the Hubble constant was known only to within a factor of two, but with the new Cepheid observations the uncertainty in the distance scale of the Universe has dropped to roughly 10%.

## The life cycle of stars

Although stars are frequently assumed to be constant and unchanging features of the firmament, they are in fact evolving dynamic systems. New stars condense out of gaseous nebulae, and old stars evolve through planetary nebulae and supernovae into white dwarfs, neutron stars and black holes. These processes—star formation and evolution—are critical to understanding many features of the Universe, including the evolution of galaxies, the dispersal of chemical elements and the distribution and energetics of gas.

Some of the HST's most lasting (and beautiful) contributions to stellar astronomy have been its studies of star-forming regions like the Orion nebula (Fig. 3). In these regions, luminous massive stars ionize the gas cloud from which they coalesced, causing the cloud to glow brightly in various emission lines. The HST's earliest observations of the Orion nebula[3,4] revealed that it was peppered with a remarkable population of young stars surrounded by dense disks of gas and dust. These disks are undoubtedly remnants of the late accretion phase during which the stars condensed. Although the presence of such disks had been inferred from theory[5] and from observations with the Very Large Array[6], the HST's superior image resolution revealed the first true pictures of the disks' structures and physical properties.

The observed 'proto-planetary disks' are exactly the type of system that astronomers expect will evolve into planetary systems like those hosted by our own Sun. The ubiquity of the disks seen in the HST images gave strong hints that our Solar System is unlikely to be unique, and recent studies have indeed found direct evidence for the 'extrasolar' planetary systems that are expected to evolve from the disks seen in the images. The HST is studying intermediate stages of this process directly, by mapping the detailed structures of disks that have lost their gas but are still dominated by dust that will eventually be either incorporated into planets or dispersed[7–10]. Although individual cases had been observed from the ground, the HST has proven the ubiquity of such systems. Moreover, with its superb resolution, the HST is uncovering evidence of structure in these debris disks, indicating that they have been shaped by the gravitational influence of planets orbiting the young, distant host stars[11].

In addition to revealing the properties of young stars, the HST continues to help us understand the older stars that dominate the stellar content of our Galaxy. Although many of these stars are relatively ordinary stars like the Sun, the majority are much fainter and are of lower mass. At these low masses, the stars begin to have more in common with planets, hosting complex atmospheres and sometimes lacking a central energy source (brown dwarfs). Luckily, many of these stars are also locked into gravitationally bound orbiting pairs, known as binaries, which serve as laboratories for measuring of the properties of stars. The orbits of binary stars can be used to derive their masses, and, because the stars in the binary can be assumed to have formed simultaneously, it can also be assumed that they have a common age and metallicity. Binaries are thus particularly useful when studying poorly understood types of star. Unfortunately, most stars are far enough away that the images of the two stars in the binary cannot be separated in a typical image, making it difficult to measure the orbits, luminosities, colours and spectra of the two components. This step is particularly difficult when one of the stars is much fainter than the other, as is common for low-mass stars, which are among the most complex and least well-understood of normal stars. However, with the HST's spatial resolution, image stability and low background, the properties of binary stars can easily be measured. The HST has thus powered critical advances in our understanding of low-mass stars and brown dwarfs, by identifying the earliest brown dwarf binaries[12,13], characterizing the relationship between mass and luminosity for low-mass stars[14], making dynamical mass measurements for field brown dwarfs[15,16], finding unusual T dwarf binaries[17] and constraining the rate of binarity at the lowest stellar masses[18,19]. It has also been an essential tool in simply quantifying the numbers of the lowest mass stars and failed brown dwarfs, both in young[20,21] and old[22,23] stellar clusters.

The HST is yielding surprises even for more ordinary stars. For most of the past century, astronomers believed that the simplest collections of stars could be found in globular clusters, which are dense, gravitationally bound groups of $\sim 10^4$–$10^6$ stars. The stars in globular clusters were thought to have formed at exactly the same time, from a single cloud of gas, giving them identical ages and chemical compositions. Unfortunately, our ability to measure the properties of individual stars in globular clusters is compromised by the high stellar densities within the clusters, and only with the HST can individual stars be separated from one another in an image. Recently, the exceptional photometric stability and high resolution of the HST have revealed that some globular clusters have far more complex properties than were previously thought possible: some host stars that formed in multiple events and/or with distinct chemical compositions[24,25]. Although this work is new, it has already begun overturning half a century of thought on the nature of these supposedly 'simple' systems.

## The death of stars

After their life of quiescent hydrogen burning is over, stars undergo dramatic changes. When the primary energy source at the centre of a star becomes exhausted, the star is forced to undergo dramatic evolution. During this evolution, the star expands drastically, sheds much of its mass and either explodes or fades away, leaving behind a bizarre stellar remnant (such as a white dwarf, neutron star or black hole).

These late phases of stellar evolution are surprisingly brief on typical astronomical timescales. Astronomers have used the HST to track the final stages of mass loss in rapidly evolving stars like $\eta$ Carinae, using time-resolved measurements to watch the expansion of the stellar ejecta in real time[26–28]. They have also revealed the ghosts of past mass ejection from evolving stars like V838 Monocerotis (ref. 29) or from SN 1987A (refs 30–32) using 'light echoes' that have bounced off expanding shells of matter ejected farther and farther into the recent past. Equally striking are the HST images of planetary nebulae[33], formed after most mass loss is complete in lower mass stars. Like the images of $\eta$ Carinae and V838 Monocerotis, the planetary nebulae show a rich level of complexity[34–36], some of which varies over year-long timescales[37,38]. Most importantly, in almost none of these cases does the distribution of ejected mass look spherical, in spite of the nearly spherical shape of the initial star. This asymmetry suggests that the process of mass loss in stars is complex, and involves 'shaping' of the stellar winds by rotation, magnetic fields and/or orbiting stellar companions.

Similar evidence that even apparently symmetric stars have asymmetric deaths comes from HST identifications of neutron stars, which are incredibly dense stellar remnants left behind after the supernova explosion of a massive star. Although they begin their lives as stars larger than the Sun, neutron stars are only a few kilometres across, making them very faint at optical wavelengths. The optical emission provides a critical means of constraining their temperatures and sizes, which in turn tells a great deal about the strange nuclear matter within the stars. The HST has been able to identify the optical counterparts of several neutron stars, and through repeated observations has found that some are hurtling through the galaxy at a surprisingly high speed of more than $100\,km\,s^{-1}$ (ref. 39). These observations suggest that the supernova somehow gives the dense stellar remnant a tremendous 'kick', shooting it out of the supernova, despite the initial star being essentially spherical.

The HST is also shedding light on the connection between supernovae from dying stars and mysterious $\gamma$-ray bursts. At the HST's launch, it was not known if these fast bursts of intense $\gamma$-ray radiation were from sources inside our galaxy or far outside it. Subsequent satellites showed that they were occurring outside our galaxy, and HST observations of the fading optical transients further localized some of the bursts to individual galaxies, in regions containing young, massive stars[40–42]. HST thus convincingly showed that these highly energetic events are tied to the very last phases of the lives of massive stars. The theoretical models resulting from these observations are suggesting that such 'hypernovae' may be essential for establishing the unusual elemental abundance patterns seen in the oldest stars.

## Black holes

The same explosions that lead to supernovae and $\gamma$-ray bursts can also lead to the formation of remnant black holes. These enigmatic objects form when mass collapses to within an extremely small radius, known as the Schwarzschild radius. For a star like the Sun to turn into a black hole, it would need to shrink by a factor of more than 200,000, down to a radius of less than 3 km. When a massive star runs out of fuel it collapses to within its Schwarzschild radius, becoming sufficiently dense that even light cannot escape from the tremendous gravitation field, and leading to the name 'black hole'. In spite of their name, black holes can be responsible for some of the most luminous astrophysical phenomena, owing to the high temperatures of the material that they sometimes accrete. However, in many cases black holes are truly dark, and their presence can only be inferred from their gravitational influence on the material around them.

Key to finding a dark black hole is to look for evidence of a large amount of mass being in a very small space. We can deduce that mass is present by the motions produced by the gravitational pull of the black hole. When these motions are very fast, and show rapid changes in velocity and/or direction over a very small distance, then we can infer the presence of a black hole. However, we need measurements of velocities that probe exceptionally small physical distances to ensure that the measured mass is in a small enough volume that it can be explained only by a black hole. Finding black holes in even the nearest galaxies thus requires the exceptional angular resolution of the HST.

Over the past several decades, the HST has revolutionized our view of black holes and the role they have in galaxy formation. At the launch of the HST, it was generally assumed that supermassive black holes were needed to explain the unusually high luminosities and peculiar spectra of distant quasi-stellar objects (QSOs) and lower luminosity nearby active galactic nuclei. However, there was then no firm evidence that QSOs were always hosted by galaxies, or that all galaxies currently hosted remnant black holes left over from an early epoch when QSOs were common. Some ground-based observations strongly suggested that a handful of the nearest galaxies might host dense, massive objects at their centres, but the identification of these as black holes was far from confirmed[43].

Since its launch, the HST has been engaged in a systematic observational assault on these issues. One of the earliest HST Key Projects was responsible for establishing that all QSOs (which were thought be powered by black holes) were indeed hosted by galaxies[44]. Later, dynamical modelling of HST spectra in nearby galaxies confirmed the presence of black holes through their gravitational influence on the surrounding stars[45–48]. These studies led to dozens of robust measurements of central black hole masses, which then revealed an extremely tight correlation between black hole mass and the mass of the galactic bulge (the smooth, rounded stellar component at the galaxy's centre)[49,50]; this relationship had been hinted at in previous ground-based work, but with much larger uncertainty and scatter. Moreover, the modelling showed that even dormant galaxies without luminous active nuclei—a sign of accretion onto a black hole—also hosted black holes, confirming that central, massive black holes are a generic feature of galaxy formation.

This surprising result has yet to be understood. The black holes that form during the deaths of massive stars have relatively small masses, and are unlikely to be more than 20 times more massive than the Sun. By contrast, black holes at the centres of galaxies are millions or billions of times more massive than the Sun, leaving open questions about how the supermassive black holes formed, how they migrated to the centre and how their masses 'knew' about the masses of their host galaxies. HST observations are beginning to unravel some of these questions, hinting that intermediate, $\sim 10^4$-solar-mass, black holes might exist in some globular clusters[51,52] that could later accrete into the galactic centre, but that some bulgeless galaxies (like our neighbour M33) have no evidence for a central black hole at all[53]. The HST's resolution has also been essential to the observation of structures that may be either analogues or precursors of central black holes. These 'nuclear clusters' are dense stellar knots found at the centres of some galaxies. The masses of nuclear clusters are also correlated with galaxy properties[54–56], raising the suspicion that they are potentially visible manifestations of the processes that may lead to supermassive black holes. The HST has shown that at least some of these clusters are disk-like, suggesting that gas accretion may have a role in the growth of massive structures at the centres of galaxies[57].

Given the presence of massive black holes at the centres of most galaxies, it might be expected that the black holes have helped to shape the distribution of stars around them. Such an effect should be strongest in massive galaxies, owing to the more massive black holes within. Indeed, some of the earliest investigations with the HST revealed strong differences between the central stellar distributions of massive and low-mass galaxies[58,59]; these differences, although recently questioned[60], have been confirmed in many subsequent studies[61–63]. Galaxies were found to have a sharp bimodality at their centres, with the more massive galaxies having flat 'cores' in their light distributions and lower mass galaxies having a bright central cusp. Some models predict that these flat cores could be produced by pairs of central black holes, the orbits of which can fling stars out of the galactic centres[64] either before or during merging. Although the observed trend can be interpreted as a response to the presence of central black holes, there are many other properties of the galaxies that similarly correlate with the central light profile, such as the overall shape of the galaxy (box-like versus disk-like, triaxial versus axisymmetric) and the internal kinetics (rotating versus non-rotating). These trends may indicate that the dichotomy between core and cusp galaxies may transcend the properties of the central black holes, and may instead be intimately linked with the formation of the galaxy as a whole.

## Growth of galaxies

At the time that the HST was launched, astronomers had long been used to seeing the familiar, regular forms of galaxies at the present day. However, there were long-standing questions as to how these forms came about, and how they may have changed and evolved through time. In principle, the question could be answered by looking at distant

galaxies, which are so far away that light emitted many billions of years ago is only now reaching us. Thus, in progressively more distant galaxies we can see earlier and earlier snapshots of the galaxies' evolution, reaching back to a time when the Universe was only a fraction of its present age—an effect much like receiving postcards sent from ever more distant places, carrying old news from the time they were sent. Unfortunately, owing to blurring produced by the Earth's atmosphere, these distant galaxies appeared only as unresolved smudges in images taken from the ground.

With the launch of the HST, astronomers got their first look at the shapes and structures of young galaxies, and what they saw was surprising (Fig. 4). Instead of looking like close analogues of the spiral and elliptical galaxies we see today, images of the distant Universe revealed a large population of galaxies that looked not unlike insects splattered on a windscreen. This population can be seen most dramatically in images of the Hubble Deep Fields[65,66] and the later-generation Ultra Deep Field[67], made with a more sensitive, larger-format camera.

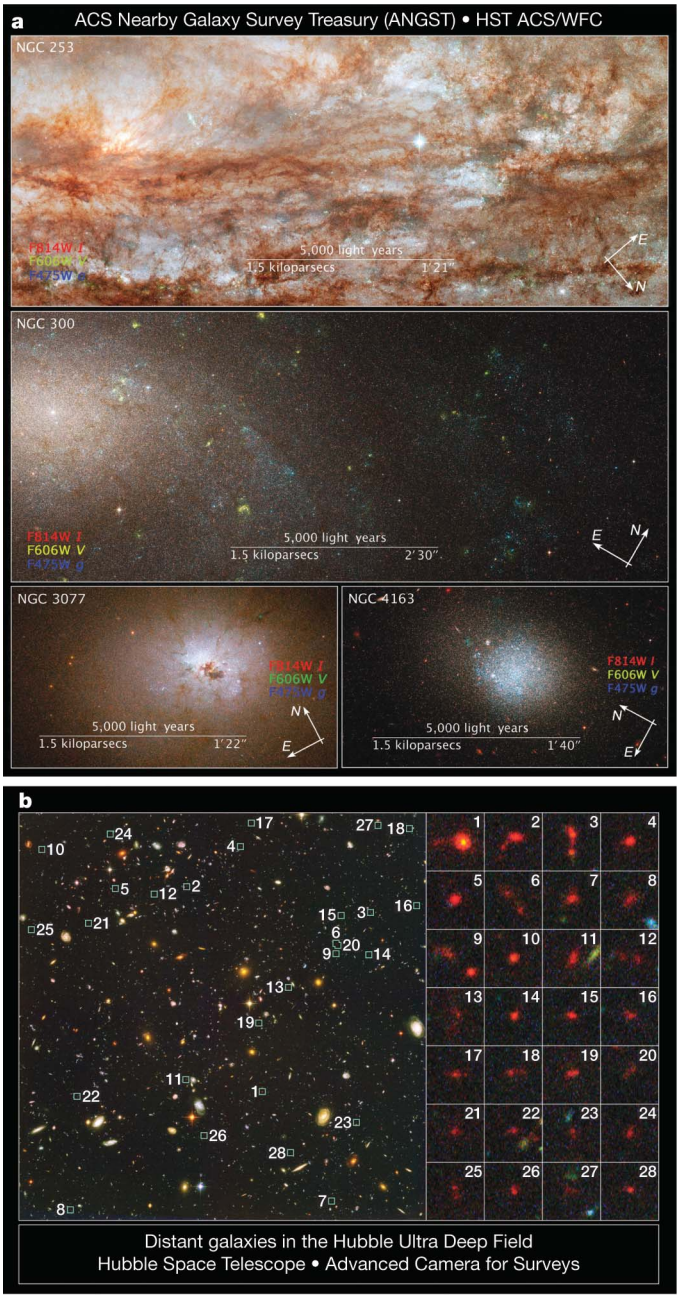


**Figure 4 | Galaxies near and far. a**, Images showing the diverse properties of galaxies. **b**, Unusually shaped distant galaxies in the Hubble Ultra Deep Field. Images courtesy of NASA.

The HST deep field images revealed that young galaxies were built out of fragments, through a process that we now understand to be the hierarchical build-up of smaller galaxies into ever larger ones. The HST images were key in establishing the current galaxy formation model, in which galaxy properties are shaped by the continual merger and accretion of matter over cosmic timescales[68–74]. Parallel work in clusters of galaxies showed the influence of merging on larger scales, using the combination of HST images and spectroscopy[75–82]. Only with the HST could we measure the complicated structures and sizes[83,84] of these younger evolving galaxies.

Also key in establishing this change in model was the huge investment made in measuring relative distances to the galaxies in the Hubble Deep Field (HDF). Measuring relative distances requires time-consuming spectroscopy of faint individual galaxies with which one can measure recessional velocities. Although such programmes are expensive in terms of limited telescope resources, given the unprecedented allocation of the HST's resources in producing the HDF, the astronomical community responded with an equally unprecedented investment of spectroscopic observations of the HDF galaxies[85–87]. These spectroscopic observations became key in establishing the link between a galaxy's observed colour and its distance. This 'photometric redshift' technique had been developed for nearby galaxies[88], but only with the HDF was it confirmed to be a viable method for measuring distances to the most distant galaxies[89]. Since the verification of this technique in the HDF, there has been an explosion in the use of photometric redshifts, allowing major surveys[90–93] to skip time-consuming spectroscopy when establishing the relative distances of galaxies. Photometric redshifts also allow astronomers to estimate distances to galaxies that are otherwise too faint for spectroscopic observations. Some of the earliest work applying photometric redshifts were used for the HDF itself[94–96], and showed most clearly the assembly of galaxies from small lumps into large coherent units, and the accompanying rise in the overall rate of star formation in the Universe[94,97].

In addition to the great strides made through its *in situ* studies of distant young galaxies, the HST has made equal progress using the complementary tool of studying the fossil record that galaxy formation has left behind. This record is embedded in the individual stars that formed during a galaxy's lifetime. Seen from the ground, these billions of stars blur into a single smooth image. However, when viewed at the highest spatial resolution, the smooth galaxy image breaks into millions of individual points, revealing individual stars, much like the pointillism seen in a Seurat painting. The colours and brightnesses of these stars encode information about their ages and chemical compositions[98], and allow us to infer the past history of star formation in the galaxy.

With the accurate measurements provided by the HST's spatial resolution and photometric stability, astronomers have characterized the stellar populations of the oldest extended structures in galaxies[99–106], tracing the earliest epochs of a galaxy's assembly. They have also used the HST to map the ebb and flow of star formation across the disk of nearby galaxies, tracing the detailed evolution of star formation over hundreds of millions of years[107].

## Cosmology

Some of the most widely recognized successes of the HST have been in the field of cosmology. Cosmology attempts to measure and understand the most basic large-scale features of the Universe, such as its age, composition and size. Constraining these quantities relies primarily on astronomical observations, which are among the only tools that can access the distances and ages over which the Universe's evolution and structure can be measured.

The age of the Universe can be inferred in multiple ways. The most secure measurements of the age come from the oldest stars we see today, whose ages place a secure lower limit on the age of the Universe. To derive ages for a population of stars, we ideally want to find a cluster of stars that were all born at the same time. The stars within the cluster all evolve at different rates, such that the most

massive stars quickly become supernovae, the intermediate-mass stars (like the Sun) evolve into planetary nebulae and leave behind a faint remnant white dwarf, and the lowest mass stars last for the age of the Universe. The age of the stellar cluster can then be inferred from the masses of the stars that are left behind.

There has been an elegant series of HST measurements using this technique, focusing on white dwarfs. After a white dwarf forms, it no longer has a source of energy in its core. It therefore cools steadily, dropping in temperature and brightness at a rate that can be calculated from theoretical models. These models can be compared with the observed distribution of brightnesses to infer the age of the white dwarf, placing a robust lower limit on the age of the star[108–112]. Unfortunately, white dwarfs are sufficiently faint that they can be difficult to isolate from other stars. In a clever twist, astronomers have used repeated, deep observations with the HST to separate faint cluster stars from intervening and background objects[113–115]. The stars in the cluster all share a common velocity, causing them to show slight shifts in position between the two epochs of observation. These shifts are distinct from those shown by foreground and background stars, allowing the cluster stars to be isolated down to very faint luminosities with little confusion. The resulting measurements of the distribution of white dwarf brightnesses are tremendously precise, and have placed secure lower limits on the age of the Universe that do not depend on uncertain observations at high redshift or assumptions about the underlying cosmology. Instead, they rely solely on our understanding of the physics of stars, making this a superb independent check on a fundamental cosmological measurement. This measurement could not have been made without the high resolution and the photometric (and astrometric) stability of the HST

An independent probe of the Universe's age comes from the HST's measurement of the Hubble constant using Cepheid distances. In addition to providing a fundamental distance scale for the Universe, the value of the Hubble constant is directly related to the rate at which the Universe is expanding at the present day. Its value is therefore critical in extrapolating between the present and the Big Bang, and thus in establishing the duration of the expansion.

Whereas the Hubble constant constrains the rate of the Universe's expansion at the present day, astronomical observations can also be used to constrain the Universe's past expansion. Our understanding of the past rate of expansion has been revolutionized by the study of the brightnesses of high-redshift supernovae. Progressively more distant supernovae should be increasingly fainter, in a way that depends sensitively on the exact model of the Universe in which we live. Measurements of distant supernovae have shown that they appear unusually faint[116–122]. However, the typical luminosities of supernovae are well understood, and their apparent faintness must thus indicate that they are much farther away than had been anticipated in the early 1990s. For this to be true, the Universe must be expanding far faster than in any model that includes only relatively normal forms of matter. This evidence for 'dark energy' or 'cosmological acceleration' was one of the ground-breaking scientific discoveries of the late 1990s.

The HST has been essential in discovering and monitoring ever more distant supernovae, which probe early epochs in the Universe's expansion. At such large distances, it is difficult to measure the properties of supernovae from the ground, owing to their faintness and the blurring of their light with the surrounding galaxy. With the HST, however, the supernovae can be separated cleanly from the host galaxy, allowing the brightnesses to be measured. These precisely measured brightnesses constrain the distances to the supernovae, and limit the nature of the expansion at these early times, providing a strong limit on possible models for the nature of the dark energy.

Supernova measurements of the dark energy suggest that it dominates the mass-energy density of the Universe, but there is still an enormous quantity of dark matter pervading space. Although its true nature eludes us, its mass and distribution can be probed through indirect techniques. One of the most successful techniques is through the distortion that dark matter produces on images of background galaxies. Like looking through the bottom of a wine glass, the mass of dark matter distorts light passing through it, producing a warped image of all the images seen through the dark matter. Normally, this effect is too small to be measured, but for the densest concentrations of dark matter, found in massive clusters of galaxies, the effect can be dramatic, producing enormous arcs and ring-like structures around the clusters[123]. These images are among the most spectacular extragalactic images produced by HST.

With the precision offered by the HST's resolution, astronomers have mastered techniques that use the observed distortions to reconstruct the distribution of mass that produced them. This makes it possible to map the dark matter distribution, in spite of not being able to see it directly[124–126]. One of the most striking uses of this technique can be seen in recent observations of two colliding galaxy clusters (the 'bullet cluster'). Maps of the dark matter constructed from HST images show a remarkable separation of the dark matter from the gas in the cluster[127]. Like two colliding streams of water, the gas was essentially stopped in the collision, whereas the dark matter and the galaxies passed through. These observations are striking confirmation that the dark matter is not associated with the gas (which dominates the normal matter in the clusters), and that the dark matter acts like 'collisionless' particles that interact only through gravity and not any electromagnetic process. Thus, in spite of not knowing what the dark matter is, the HST has allowed us to learn what it is not, and how it behaves on large scales.

## Gas in the Universe

Although cosmology tells us that the majority of the mass in the Universe is hidden in the dark sector, nearly all the light we see comes from normal, familiar forms of matter. This matter is only a small fraction of the Universe's mass, but understanding what forms it takes and how it is distributed through space constrains many astrophysical questions.

The majority of normal baryonic matter is thought to be in the gas phase, and can produce both emission lines and absorption lines in astrophysical spectra. The location (in wavelength) and amplitude of these lines can be used to constrain the chemical composition, temperature, density and pressure of the gas. Although optical spectroscopy from the ground can routinely study some of the spectroscopic features produced by astrophysical gases, many of the most useful features are found at ultraviolet wavelengths, and can only be studied from space.

Ultraviolet spectroscopy with the HST has allowed astronomers to track where gas is and how the amount of matter in the gas phase has changed with time. One of the earliest HST Key Projects mapped the distribution of gas in the (relatively) nearby Universe using the absorption lines produced by hydrogen along the line of sight to more distant quasars[128]. Gas had previously been tracked in this manner, but only at larger distances that probe the properties of the Universe long ago. The evolution of the gas phase could therefore not be tracked continuously to the present, leaving the final destination of the gas uncertain. Moreover, when restricted to such large distances, little was known about exactly what astronomical objects the gas was associated with. Was it bound to galaxies? Or was it distributed in the otherwise empty volume of space between galaxies? Only with the HST's ultraviolet sensitivity could the amount and distribution of this gas be tracked to the present day, through the local distribution of galaxies. The HST thus made it possible to follow the evolution of the primary gas reservoir in the Universe from the earliest times to the present[129–132] and, moreover, to match the gas seen in absorption to other nearby galaxies[133–138]. These early studies showed that there was rapid evolution in the amount of broadly distributed gas, as it was absorbed into galaxies, and that there were multiple populations of absorbing clouds, some that were clearly associated with galaxies and others that resided in the 'cosmic web'. More recently, ultraviolet spectroscopy with the HST has

uncovered an even larger reservoir of gas[139], which simulations[140] and subsequent ultraviolet observations with NASA's Far Ultraviolet Spectroscopic Explorer[141,142] suggest is hiding in a hot, diffuse plasma surrounding nearby galaxies. This ionized gas may contain even more mass than is currently found in stars and cool gas.

In addition to tracking the broad movement of gas from the cosmic web into galaxies, the HST has been essential in tracing the detailed properties of gas within individual galaxies, and particularly within the Milky Way. Ultraviolet spectroscopy of nearby stars shows a rich network of absorption lines produced by several dozen different elements found in the gas in our galaxy. By analysing the depths of various absorption features, astronomers have shown in detail how different elements move in and out of the gas phase as they are expelled by stars and/or condense into solid dust grains[143]. Tracking these changes improves our understanding both of how these elements are produced deep within stars and of the properties of the dust which clouds almost every astronomical observation.

## A new way forward for astronomy

Beyond the direct scientific impact of its observations, the HST has had a significant role in shaping the culture of astronomy. In many scientific fields, data are proprietary, and are owned indefinitely by the groups who performed an individual experiment. Ground-based astronomy was no different in this regard. The HST, however, was recognized to be a sufficiently unique and limited resource as to make an indefinite proprietary period unjustifiable. Instead, any data taken by the HST are open for anyone to use after only one year. This policy is an effective multiplier for the HST's impact, allowing all data to be used by multiple groups, for multiple purposes, facilitated by the HST's excellent archiving programme.

This movement towards non-proprietary data was greatly accelerated by the HDF, which was imaged using an unprecedented allocation of observing time donated by the director of the Space Telescope Science Institute, Bob Williams. The images were reduced by staff at the institute and released to the public immediately. The wider astronomical community responded by investing their own resources in spectroscopy and follow-up imaging at other wavelengths, using other facilities. This coming together of the community to generate a shared, non-proprietary data set was essentially unprecedented, but has since become the model for the majority of large astronomical projects. Almost all major astronomical surveys are now proposed with the expectation that the data and data products will be publicly released during the project, rather than held in perpetuity by those few who instigated the programme. This new mode of operating has democratized astronomy by opening astronomical research to scientists that are at relatively under-resourced institutions, allowing researchers at small colleges, or in poor countries, to have access to some of the finest data sets in the world. The policies established by the HST's oversight board were crucial steps in ushering in this cultural change.

## The future of the HST

Owing to the HST's upcoming servicing mission, the installation's future looks as bright as its past. With increased imaging sensitivity at ultraviolet and near-infrared wavelengths, enhanced ultraviolet spectroscopy and the restoration of several failed instruments, the HST will surpass any capability it had in the past. Even as astronomers master the art of achieving high-resolution imaging from the ground through adaptive optics, the HST's photometric stability, ultraviolet sensitivity and low background will remain unparalleled. Unfortunately, when the HST is finally decommissioned, the window of high-resolution optical and ultraviolet imaging will be sadly closed for decades to come.


1. Benedict, G. F. *et al.* Hubble Space Telescope fine guidance sensor parallaxes of Galactic Cepheid Variable stars: Period-luminosity relations. *Astron. J.* **133,** 1810–1827 (2007).
2. Kennicutt, R. C. Jr *et al.* The Hubble Space Telescope Key Project on the extragalactic distance scale. XIII. The metallicity dependence of the Cepheid distance scale. *Astrophys. J.* **498,** 181–194 (1998).
3. O'Dell, C. R., Wen, Z. & Hu, X. Discovery of new objects in the Orion nebula on HST images - Shocks, compact sources, and protoplanetary disks. *Astrophys. J.* **410,** 696–700 (1993).
4. O'Dell, C. R. & Wen, Z. Postrefurbishment mission Hubble Space Telescope images of the core of the Orion Nebula: Proplyds, Herbig-Haro objects, and measurements of a circumstellar disk. *Astrophys. J.* **436,** 194–202 (1994).
5. Shu, F. H., Adams, F. C. & Lizano, S. Star formation in molecular clouds - Observation and theory. *Annu. Rev. Astron. Astrophys.* **25,** 23–81 (1987).
6. Felli, M., Churchwell, E., Wilson, T. L. & Taylor, G. B. The radio continuum morphology of the Orion Nebula - From 10 arcmin to 0.1 arcsec resolution. *Astron. Astrophys. Suppl. Ser.* **98,** 137–164 (1993).
7. Schneider, G. *et al.* NICMOS imaging of the HR 4796A circumstellar disk. *Astrophys. J.* **513,** L127–L130 (1999).
8. Heap, S. R. *et al.* Space Telescope Imaging Spectrograph coronagraphic observations of $\beta$ Pictoris. *Astrophys. J.* **539,** 435–444 (2000).
9. Krist, J. E. *et al.* Hubble Space Telescope Advanced Camera for Surveys coronagraphic imaging of the AU Microscopii debris disk. *Astron. J.* **129,** 1008–1017 (2005).
10. Golimowski, D. A. *et al.* Hubble Space Telescope ACS multiband coronagraphic imaging of the debris disk around $\beta$ Pictoris. *Astron. J.* **131,** 3109–3130 (2006).
11. Kalas, P., Graham, J. R. & Clampin, M. A planetary system as the origin of structure in Fomalhaut's dust belt. *Nature* **435,** 1067–1070 (2005).
12. Martin, E. L., Brandner, W. & Basri, G. A search for companions to nearby brown dwarfs: The binary DENIS-P J1228.2-1547. *Science* **283,** 1718–1720 (1999).
13. Lowrance, P. J. *et al.* A candidate substellar companion to CD -33 deg7795 (TWA 5). *Astrophys. J.* **512,** L69–L72 (1999).
14. Henry, T. J. *et al.* The optical mass-luminosity relation at the end of the main sequence (0.08 - 0.20$M_{\odot}$). *Astrophys. J.* **512,** 864–873 (1999).
15. Bouy, H. *et al.* First determination of the dynamical mass of a binary L dwarf. *Astron. Astrophys.* **423,** 341–352 (2004).
16. Golimowski, D. A., Burrows, C. J., Kulkarni, S. R., Oppenheimer, B. R. & Brukardt, R. A. Wide Field Planetary Camera 2 observations of the brown dwarf Gliese 229B: Optical colors and orbital motion. *Astron. J.* **115,** 2579–2586 (1998).
17. Burgasser, A. J. *et al.* Binarity in brown dwarfs: T dwarf binaries discovered with the Hubble Space TelescopeWide Field Planetary Camera 2. *Astrophys. J.* **586,** 512–526 (2003).
18. Martín, E. L. *et al.* Membership and multiplicity among very low mass stars and brown dwarfs in the Pleiades cluster. *Astrophys. J.* **543,** 299–312 (2000).
19. Allen, P. R. Star formation via the little guy: A Bayesian study of ultracool dwarf imaging surveys for companions. *Astrophys. J.* **668,** 492–506 (2007).
20. Luhman, K. L. *et al.* The initial mass function of low-mass stars and brown dwarfs in young clusters. *Astrophys. J.* **540,** 1016–1040 (2000).
21. Najita, J. R., Tiede, G. P. & Carr, J. S. From stars to superplanets: The low-mass initial mass function in the young cluster IC 348. *Astrophys. J.* **541,** 977–1003 (2000).
22. King, I. R., Anderson, J., Cool, A. M. & Piotto, G. The luminosity function of the globular cluster NGC 6397 near the limit of hydrogen burning. *Astrophys. J.* **492,** L37–L40 (1998).
23. Richer, H. B. *et al.* Deep Advanced Camera for Surveys imaging in the globular cluster NGC 6397: the cluster color-magnitude diagram and luminosity function. *Astron. J.* **135,** 2141–2154 (2008).
24. Bedin, L. R. *et al.* $\omega$ Centauri: The population puzzle goes deeper. *Astrophys. J.* **605,** L125–L128 (2004).
25. Piotto, G. *et al.* A triple main sequence in the globular cluster NGC 2808. *Astrophys. J.* **661,** L53–L56 (2007).
26. Currie, D. G. *et al.* Astrometric analysis of the homunculus of eta Carinae with the Hubble Space Telescope. *Astron. J.* **112,** 1115–1127 (1996).
27. Morse, J. A. *et al.* Hubble Space Telescope proper-motion measurements of the $\eta$ Carinae Nebula. *Astrophys. J.* **548,** L207–L211 (2001).
28. O'Dell, C. R. & Doi, T. High proper motion features in the central Orion nebula. *Astron. J.* **125,** 277–287 (2003).
29. Bond, H. E. *et al.* An energetic stellar outburst accompanied by circumstellar light echoes. *Nature* **422,** 405–408 (2003).
30. Jakobsen, P. *et al.* First results from the Faint Object Camera - SN 1987A. *Astrophys. J.* **369,** L63–L66 (1991).
31. Burrows, C. J. *et al.* Hubble Space Telescope observations of the SN 1987A triple ring nebula. *Astrophys. J.* **452,** 680–684 (1995).
32. Plait, P. C., Lundqvist, P., Chevalier, R. A. & Kirshner, R. P. HST observations of the ring around SN 1987A. *Astrophys. J.* **439,** 730–751 (1995).
33. Balick, B. & Frank, A. Shapes and shaping of planetary nebulae. *Annu. Rev. Astron. Astrophys.* **40,** 439–486 (2002).
34. Sahai, R. & Trauger, J. T. Multipolar bubbles and jets in low-excitation planetary nebulae: Toward a new understanding of the formation and shaping of planetary nebulae. *Astron. J.* **116,** 1357–1366 (1998).
35. Balick, B. *et al.* FLIERs and other microstructures in planetary nebulae. IV. Images of elliptical PNs from the Hubble Space Telescope. *Astron. J.* **116,** 360–371 (1998).
36. O'Dell, C. R., Balick, B., Hajian, A. R., Henney, W. J. & Burkert, A. Knots in nearby planetary nebulae. *Astron. J.* **123,** 3329–3347 (2002).
37. Reed, D. S. *et al.* Hubble Space Telescope measurements of the expansion of NGC 6543: Parallax distance and nebular evolution. *Astron. J.* **118,** 2430–2441 (1999).

38. Fernández, R., Monteiro, H. & Schwarz, H. E. Proper motion and kinematics of the ansae in NGC 7009. *Astrophys. J.* **603,** 595–598 (2004).
39. Walter, F. M. The proper motion, parallax, and origin of the isolated neutron star RX J185635–3754. *Astrophys. J.* **549,** 433–440 (2001).
40. Fruchter, A. S. *et al.* Hubble Space Telescope and Palomar imaging of GRB 990123: Implications for the nature of gamma-ray bursts and their hosts. *Astrophys. J.* **519,** L13–L16 (1999).
41. Bloom, J. S., Kulkarni, S. R. & Djorgovski, S. G. The observed offset distribution of gamma-ray bursts from their host galaxies: A robust clue to the nature of the progenitors. *Astron. J.* **123,** 1111–1148 (2002).
42. Fruchter, A. S. *et al.* Long $\gamma$-ray bursts and core-collapse supernovae have different environments. *Nature* **441,** 463–468 (2006).
43. Kormendy, J. & Richstone, D. Inward bound? The search for supermassive black holes in galactic nuclei. *Annu. Rev. Astron. Astrophys.* **33,** 581–624 (1995).
44. Bahcall, J. N., Kirhakos, S., Saxe, D. H. & Schneider, D. P. Hubble Space Telescope images of a sample of 20 nearby luminous quasars. *Astrophys. J.* **479,** 642–658 (1997).
45. Ferrarese, L., Ford, H. C. & Jaffe, W. Evidence for a massive black hole in the active galaxy NGC 4261 from Hubble Space Telescope images and spectra. *Astrophys. J.* **470,** 444–459 (1996).
46. Kormendy, J. *et al.* Hubble Space Telescope spectroscopic evidence for a $2 \times 10^9$ $M_\odot$ black hole in NGC 3115. *Astrophys. J.* **459,** L57–L60 (1996).
47. van der Marel, R. P., Cretton, N., de Zeeuw, P. T. & Rix, H.-W. Improved evidence for a black hole in M32 from HST/FOS Spectra. II. Axisymmetric dynamical models. *Astrophys. J.* **493,** 613–631 (1998).
48. Gebhardt, K. *et al.* Axisymmetric, three-integral models of galaxies: A massive black hole in NGC 3379. *Astron. J.* **119,** 1157–1171 (2000).
49. Ferrarese, L. & Merritt, D. A fundamental relation between supermassive black holes and their host galaxies. *Astrophys. J.* **539,** L9–L12 (2000).
50. Gebhardt, K. *et al.* A relationship between nuclear black hole mass and galaxy velocity dispersion. *Astrophys. J.* **539,** L13–L16 (2000).
51. Gerssen, J. *et al.* Hubble Space Telescope evidence for an intermediate-mass black hole in the globular cluster M15. II. Kinematic analysis and dynamical modeling. *Astron. J.* **124,** 3270–3288 (2002).
52. Gebhardt, K., Rich, R. M. & Ho, L. C. A 20,000$M_\odot$ black hole in the stellar cluster G1. *Astrophys. J.* **578,** L41–L45 (2002).
53. Gebhardt, K. *et al.* M33: A galaxy with no supermassive black hole. *Astron. J.* **122,** 2469–2476 (2001).
54. Ferrarese, L. *et al.* A fundamental relation between compact stellar nuclei, supermassive black holes, and their host galaxies. *Astrophys. J.* **644,** L21–L24 (2006).
55. Wehner, E. H. & Harris, W. E. From supermassive black holes to dwarf elliptical nuclei: A mass continuum. *Astrophys. J.* **644,** L17–L20 (2006).
56. Balcells, M., Graham, A. W. & Peletier, R. F. Galactic bulges from Hubble Space Telescope NICMOS Observations: Central Galaxian objects, and nuclear profile slopes. *Astrophys. J.* **665,** 1084–1103 (2007).
57. Seth, A. C., Dalcanton, J. J., Hodge, P. W. & Debattista, V. P. Clues to nuclear star cluster formation from edge-on spirals. *Astron. J.* **132,** 2539–2555 (2006).
58. Lauer, T. R. *et al.* The centers of early-type galaxies with HST. I. An observational survey. *Astron. J.* **110,** 2622–2654 (1995).
59. Faber, S. M. *et al.* The centers of early-type galaxies with HST. IV. Central parameter relations. *Astron. J.* **114,** 1771–1796 (1997).
60. Ferrarese, L. *et al.* The ACS Virgo cluster survey. VI. Isophotal analysis and the structure of early-type galaxies. *Astrophys. J. Suppl. Ser.* **164,** 334–434 (2006).
61. Rest, A. *et al.* WFPC2 images of the central regions of early-type galaxies. I. The data. *Astron. J.* **121,** 2431–2482 (2001).
62. Ravindranath, S., Ho, L. C., Peng, C. Y., Filippenko, A. V. & Sargent, W. L. W. Central structural parameters of early-type galaxies as viewed with Nicmos on the Hubble Space Telescope. *Astron. J.* **122,** 653–678 (2001).
63. Lauer, T. R. *et al.* The centers of early-type galaxies with Hubble Space Telescope. VI. Bimodal central surface brightness profiles. *Astrophys. J.* **664,** 226–256 (2007).
64. Begelman, M. C., Blandford, R. D. & Rees, M. J. Massive black hole binaries in active galactic nuclei. *Nature* **287,** 307–309 (1980).
65. Williams, R. E. *et al.* The Hubble Deep Field: Observations, data reduction, and galaxy photometry. *Astron. J.* **112,** 1335–1389 (1996).
66. Williams, R. E. *et al.* The Hubble Deep Field South: Formulation of the observing campaign. *Astron. J.* **120,** 2735–2746 (2000).
67. Beckwith, S. V. W. *et al.* The Hubble Ultra Deep Field. *Astron. J.* **132,** 1729–1755 (2006).
68. Glazebrook, K., Ellis, R., Santiago, B. & Griffiths, R. The morphological identification of the rapidly evolving population of faint galaxies. *Mon. Not. R. Astron. Soc.* **275,** L19–L22 (1995).
69. Abraham, R. G. *et al.* Galaxy morphology to I=25 mag in the Hubble Deep Field. *Mon. Not. R. Astron. Soc.* **279,** L47–L52 (1996).
70. Odewahn, S. C., Windhorst, R. A., Driver, S. P. & Keel, W. C. Automated morphological classification in deep Hubble Space Telescope UBVI fields: Rapidly and passively evolving faint galaxy populations. *Astrophys. J.* **472,** L13–L16 (1996).
71. Driver, S. P., Windhorst, R. A. & Griffiths, R. E. The contribution of late-type/irregulars to the faint galaxy counts from Hubble Space Telescope Medium-Deep Survey images. *Astrophys. J.* **453,** 48–64 (1995).
72. Giavalisco, M., Steidel, C. C. & Macchetto, F. D. Hubble Space Telescope imaging of star-forming galaxies at redshifts $Z > 3$. *Astrophys. J.* **470,** 189–194 (1996).
73. van Dokkum, P. G., Franx, M., Kelson, D. D. & Illingworth, G. D. Luminosity evolution of early-type galaxies to $Z = 0.83$: Constraints on formation epoch and Omega. *Astrophys. J.* **504,** L17–L21 (1998).
74. Le Fèvre, O. *et al.* Hubble Space Telescope imaging of the CFRS and LDSS redshift surveys - IV. Influence of mergers in the evolution of faint field galaxies from $z \sim 1$. *Mon. Not. R. Astron. Soc.* **311,** 565–575 (2000).
75. Dressler, A., Oemler, A. J., Butcher, H. R. & Gunn, J. E. The morphology of distant cluster galaxies. 1: HST observations of CL 0939+4713. *Astrophys. J.* **430,** 107–120 (1994).
76. Dressler, A. *et al.* Evolution since $Z = 0.5$ of the morphology-density relation for clusters of galaxies. *Astrophys. J.* **490,** 577–591 (1997).
77. Ellis, R. S. *et al.* The homogeneity of spheroidal populations in distant clusters. *Astrophys. J.* **483,** 582–596 (1997).
78. Stanford, S. A., Eisenhardt, P. R. & Dickinson, M. The evolution of early-type galaxies in distant clusters. *Astrophys. J.* **492,** 461–479 (1998).
79. Couch, W. J., Barger, A. J., Smail, I., Ellis, R. S. & Sharples, R. M. Morphological studies of the galaxy populations in distant 'Butcher-Oemler' clusters with the Hubble Space Telescope. II. AC 103, AC 118, and AC 114 at $Z = 0.31$. *Astrophys. J.* **497,** 188–211 (1998).
80. Postman, M., Lubin, L. M. & Oke, J. B. A study of nine high-redshift clusters of galaxies. II. Photometry, spectra, and ages of clusters 0023+0423 and 1604+4304. *Astron. J.* **116,** 560–583 (1998).
81. van Dokkum, P. G., Franx, M., Fabricant, D., Kelson, D. D. & Illingworth, G. D. A high merger fraction in the rich cluster MS 1054–03 at $Z = 0.83$: Direct evidence for hierarchical formation of massive galaxies. *Astrophys. J.* **520,** L95–L98 (1999).
82. Balogh, M. L. *et al.* Distinguishing local and global influences on galaxy morphology: A Hubble Space telescope comparison of high and low x-ray luminosity clusters. *Astrophys. J.* **566,** 123–136 (2002).
83. Lilly, S. *et al.* Hubble Space Telescope imaging of the CFRS and LDSS redshift surveys. II. Structural parameters and the evolution of disk galaxies to Z approximately 1. *Astrophys. J.* **500,** 75–94 (1998).
84. Simard, L. *et al.* The magnitude-size relation of galaxies out to $z \sim 1$. *Astrophys. J.* **519,** 563–579 (1999).
85. Lowenthal, J. D. *et al.* Keck spectroscopy of redshift Z approximately 3 Galaxies in the Hubble Deep Field. *Astrophys. J.* **481,** 673–688 (1997).
86. Steidel, C. C., Giavalisco, M., Dickinson, M. & Adelberger, K. L. Spectroscopy of Lyman break galaxies in the Hubble Deep Field. *Astron. J.* **112,** 352–358 (1996).
87. Guzman, R. *et al.* The nature of compact galaxies in the Hubble Deep Field. II. Spectroscopic properties and implications for the evolution of the star formation rate density of the Universe. *Astrophys. J.* **489,** 559–572 (1997).
88. Connolly, A. J. *et al.* Slicing through multicolor space: Galaxy redshifts from broadband photometry. *Astron. J.* **110,** 2655–2664 (1995).
89. Hogg, D. W. *et al.* A blind test of photometric redshift prediction. *Astron. J.* **115,** 1418–1422 (1998).
90. Giavalisco, M. *et al.* The Great Observatories Origins Deep Survey: Initial results from optical and near-infrared imaging. *Astrophys. J.* **600,** L93–L98 (2004).
91. Rix, H.-W. *et al.* GEMS: Galaxy evolution from morphologies and SEDs. *Astrophys. J. Suppl. Ser.* **152,** 163–173 (2004).
92. Davis, M. *et al.* The All-Wavelength Extended Groth Strip International Survey (AEGIS) data sets. *Astrophys. J.* **660,** L1–L6 (2007).
93. Scoville, N. *et al.* The Cosmic Evolution Survey (COSMOS): Overview. *Astrophys. J. Suppl. Ser.* **172,** 1–8 (2007).
94. Connolly, A. J., Szalay, A. S., Dickinson, M., Subbarao, M. U. & Brunner, R. J. The evolution of the global star formation history as measured from the Hubble Deep Field. *Astrophys. J.* **486,** L11–L14 (1997).
95. Sawicki, M. J., Lin, H. & Yee, H. K. C. Evolution of the Galaxy population based on photometric redshifts in the Hubble Deep Field. *Astron. J.* **113,** 1–12 (1997).
96. Fernández-Soto, A., Lanzetta, K. M. & Yahil, A. A new catalog of photometric redshifts in the Hubble Deep Field. *Astrophys. J.* **513,** 34–50 (1999).
97. Madau, P. *et al.* High-redshift galaxies in the Hubble Deep Field: colour selection and star formation history to $z \sim 4$. *Mon. Not. R. Astron. Soc.* **283,** 1388–1404 (1996).
98. Gallart, C., Zoccali, M. & Aparicio, A. The adequacy of stellar evolution models for the interpretation of the color-magnitude diagrams of resolved stellar populations. *Annu. Rev. Astron. Astrophys.* **43,** 387–434 (2005).
99. Holland, S., Fahlman, G. G. & Richer, H. B. Deep HST V- and I-Band observations of the halo of M31: Evidence for multiple stellar populations. *Astron. J.* **112,** 1035–1045 (1996).
100. Brown, T. M. *et al.* Evidence of a significant intermediate-age population in the M31 halo from main-sequence photometry. *Astrophys. J.* **592,** L17–L20 (2003).
101. Brown, T. M. *et al.* The detailed star formation history in the spheroid, outer disk, and tidal stream of the Andromeda galaxy. *Astrophys. J.* **652,** 323–353 (2006).
102. Brown, T. M. *et al.* The extended star formation history of the Andromeda spheroid at 21 kpc on the minor axis. *Astrophys. J.* **658,** L95–L98 (2007).
103. Harris, G. L. H., Harris, W. E. & Poole, G. B. The metallicity distribution in the halo stars of NGC 5128: Implications for galaxy formation. *Astron. J.* **117,** 855–867 (1999).
104. Harris, W. E. & Harris, G. L. H. The halo stars in NGC 5128. III. An inner halo field and the metallicity distribution. *Astron. J.* **123,** 3108–3123 (2002).
105. Barker, M. K., Sarajedini, A., Geisler, D., Harding, P. & Schommer, R. The stellar populations in the outer regions of M33. III. Star formation history. *Astron. J.* **133,** 1138–1160 (2007).

106. Williams, B. F. *et al.* The ACS Nearby Galaxy Survey Treasury I. The star formation history of the M81 outer disk. Preprint at ⟨http://arxiv1.library.cornell.edu/abs/0810.2557⟩ (2008).
107. Dohm-Palmer, R. C. *et al.* Deep Hubble Space Telescope imaging of Sextans A. I. The spatially resolved recent star formation history. *Astron. J.* **123,** 813–831 (2002).
108. Richer, H. B. *et al.* White dwarfs in globular clusters: Hubble Space Telescope observations of M4. *Astrophys. J.* **484,** 741–760 (1997).
109. Calamida, A. *et al.* On the white dwarf cooling sequence of the globular cluster $\omega$ Centauri. *Astrophys. J.* **673,** L29–L33 (2008).
110. Hansen, B. M. S. *et al.* The white dwarf cooling sequence of the globular cluster Messier 4. *Astrophys. J.* **574,** L155–L158 (2002).
111. Cool, A. M., Piotto, G. & King, I. R. The main sequence and a white dwarf sequence in the globular cluster NGC 6397. *Astrophys. J.* **468,** 655–662 (1996).
112. Hansen, B. M. S. *et al.* Hubble Space Telescope observations of the white dwarf cooling sequence of M4. *Astrophys. J. Suppl. Ser.* **155,** 551–576 (2004).
113. Bedin, L. R. *et al.* The white dwarf cooling sequence in NGC 6791. *Astrophys. J.* **624,** L45–L48 (2005).
114. Hansen, B. M. S. *et al.* The white dwarf cooling sequence of NGC 6397. *Astrophys. J.* **671,** 380–401 (2007).
115. Bedin, L. R. *et al.* Reaching the end of the white dwarf cooling sequence in NGC 6791 *Astrophys. J.* **678,** 1279–1291 (2008).
116. Perlmutter, S. *et al.* Measurements of the cosmological parameters Omega and Lambda from the first seven supernovae at z ≥ 0.35. *Astrophys. J.* **483,** 565–581 (1997).
117. Riess, A. G. *et al.* Observational evidence from supernovae for an accelerating universe and a cosmological constant. *Astron. J.* **116,** 1009–1038 (1998).
118. Garnavich, P. M. *et al.* Supernova limits on the cosmic equation of state. *Astrophys. J.* **509,** 74–79 (1998).
119. Perlmutter, S. *et al.* Measurements of Omega and Lambda from 42 high-redshift supernovae. *Astrophys. J.* **517,** 565–586 (1999).
120. Riess, A. G. *et al.* The farthest known supernova: Support for an accelerating universe and a glimpse of the epoch of deceleration. *Astrophys. J.* **560,** 49–71 (2001).
121. Knop, R. A. *et al.* New constraints on $\Omega_M$, $\Omega_\lambda$ and w from an independent set of 11 high-redshift supernovae observed with the Hubble Space Telescope. *Astrophys. J.* **598,** 102–137 (2003).
122. Riess, A. G. *et al.* Type Ia supernova discoveries at z > 1 from the Hubble Space Telescope: Evidence for past deceleration and constraints on dark energy evolution. *Astrophys. J.* **607,** 665–687 (2004).
123. Kneib, J.-P., Ellis, R. S., Smail, I., Couch, W. J. & Sharples, R. M. Hubble Space Telescope observations of the lensing cluster Abell 2218. *Astrophys. J.* **471,** 643–656 (1996).
124. Squires, G. *et al.* The dark matter, gas, and galaxy distributions in Abell 2218: A weak gravitational lensing and X-ray analysis. *Astrophys. J.* **461,** 572–586 (1996).
125. Hoekstra, H., Franx, M., Kuijken, K. & Squires, G. Weak lensing analysis of CL 1358+62 using Hubble Space Telescope observations. *Astrophys. J.* **504,** 636–660 (1998).
126. Hoekstra, H., Franx, M. & Kuijken, K. Hubble Space Telescope weak-lensing study of the z=0.83 cluster MS 1054–03. *Astrophys. J.* **532,** 88–108 (2000).
127. Clowe, D. *et al.* A direct empirical proof of the existence of dark matter. *Astrophys. J.* **648,** L109–L113 (2006).
128. Bahcall, J. N. *et al.* The Hubble Space Telescope quasar absorption line key project. I – First observational results, including Lyman-alpha and Lyman-limit systems. *Astrophys. J. Suppl. Ser.* **87,** 1–43 (1993).
129. Morris, S. L., Weymann, R. J., Savage, B. D. & Gilliland, R. L. First results from the Goddard High-Resolution Spectrograph - The Galactic halo and the Ly-alpha forest at low redshift in 3C 273. *Astrophys. J.* **377,** L21–L24 (1991).
130. Penton, S. V., Stocke, J. T. & Shull, J. M. The local Ly$\alpha$ forest. IV. Space Telescope Imaging Spectrograph G140M spectra and results on the distribution and baryon content of H I absorbers. *Astrophys. J. Suppl. Ser.* **152,** 29–62 (2004).
131. Williger, G. M. *et al.* The low-redshift Ly$\alpha$ forest toward PKS 0405–123. *Astrophys. J.* **636,** 631–653 (2006).
132. Lehner, N. *et al.* Physical properties, baryon content, and evolution of the Ly$\alpha$ Forest: New insights from high-resolution observations at z ≥ 0:4. *Astrophys. J.* **658,** 680–709 (2007).
133. Lanzetta, K. M., Bowen, D. V., Tytler, D. & Webb, J. K. The gaseous extent of galaxies and the origin of Lyman-alpha absorption systems: A survey of galaxies in the fields of Hubble Space Telescope spectroscopic target QSOs. *Astrophys. J.* **442,** 538–568 (1995).
134. Stocke, J. T., Shull, J. M., Penton, S., Donahue, M. & Carilli, C. The local LY alpha forest: Association of clouds with superclusters and voids. *Astrophys. J.* **451,** 24–43 (1995).
135. Le Brun, V., Bergeron, J., Boisse, P. & Deharveng, J. M. The nature of intermediate-redshift damped Ly$\alpha$ absorbers. *Astron. Astrophys.* **321,** 733–748 (1997).
136. Steidel, C. C., Dickinson, M., Meyer, D. M., Adelberger, K. L. & Sembach, K. R. Quasar absorbing galaxies at z ≥ 1. I. Deep imaging and spectroscopy in the field of 3C 336. *Astrophys. J.* **480,** 568–588 (1997).
137. Chen, H.-W., Lanzetta, K. M., Webb, J. K. & Barcons, X. The gaseous extent of galaxies and the origin of Ly alpha absorption systems. III. Hubble Space Telescope imaging of Ly alpha-absorbing galaxies at z<1. *Astrophys. J.* **498,** 77–94 (1998).
138. Tripp, T. M., Lu, L. & Savage, B. D. The relationship between galaxies and low-redshift weak Ly alpha absorbers in the directions of H1821+643 and PG 1116+215. *Astrophys. J.* **508,** 200–231 (1998).
139. Tripp, T. M., Savage, B. D. & Jenkins, E. B. Intervening O VI quasar absorption systems at low redshift: A significant baryon reservoir. *Astrophys. J.* **534,** L1–L5 (2000).
140. Davé, R. *et al.* Baryons in the warm-hot intergalactic medium. *Astrophys. J.* **552,** 473–483 (2001).
141. Sembach, K. R. *et al.* Highly ionized high-velocity gas in the vicinity of the Galaxy. *Astrophys. J. Suppl. Ser.* **146,** 165–208 (2003).
142. Nicastro, F. *et al.* The far-ultraviolet signature of the 'missing' baryons in the Local Group of galaxies. *Nature* **421,** 719–721 (2003).
143. Savage, B. D. & Sembach, K. R. Interstellar abundances from absorption-line observations with the Hubble Space Telescope. *Annu. Rev. Astron. Astrophys.* **34,** 279–330 (1996).

**Acknowledgements** The author is happy to acknowledge many discussions with her colleagues, including H.-W. Rix, E. Bell, D. Hogg, A. Burgasser, G. Laughlin, S. Anderson, N. Reid, D. Schneider, D. Soderblom, S. Sigurdsen, J. Rigby, P. Plait, M. Livio, J. Wisniewski, and the readers of Cosmic Variance. She also thanks the staff at the Max-Planck-Institut für Astronomie for their hospitality while this article was being written.

**Author Information** Reprints and permissions information is available at www.nature.com/reprints. Correspondence should be addressed to J.D. (jd@astro.washington.edu).